Neutron diffraction study of the influence of structural disorder on the magnetic properties of Sr_2FeMO_6 (M = Ta, Sb)

Edmund J. Cussen,[a] Jaap F. Vente,[a] Peter D. Battle*[a] and Terence C. Gibb[b]

[a]*Inorganic Chemistry Laboratory, University of Oxford, South Parks Road, Oxford, UK OX1 3QR*
[b]*School of Chemistry, Leeds University, Leeds, UK LS2 9JT*

The crystal structure of the perovskite Sr_2FeTaO_6 has been refined by simultaneous analysis of X-ray and neutron powder diffraction data collected at 280 K; space group *Pbnm*, $a = 5.6204(3)$, $b = 5.6161(3)$, $c = 7.9266(3)$ Å. The structure is of the $GdFeO_3$ type, with a disordered distribution of Fe and Ta over the six-coordinate cation sites. The structure of Sr_2FeSbO_6 has been refined in a similar manner; space group $P2_1/n$, $a = 5.6132(5)$, $b = 5.5973(5)$, $c = 7.9036(7)$ Å, $\beta = 90.01(1)^\circ$. The two crystallographically distinct six-coordinate sites in Sr_2FeSbO_6 are occupied in a partially ordered manner [0.795(6):0.205(6)] by Fe and Sb atoms. Neutron diffraction data collected from Sr_2FeTaO_6 at 1.5 K show no evidence of long-range magnetic ordering and, in the light of previous susceptibility and Mössbauer measurements, it is concluded that Sr_2FeTaO_6 is a spin glass below 23 K. Neutron diffraction data collected from Sr_2FeSbO_6 at 1.5 K include magnetic Bragg peaks characteristic of a type I magnetic structure with an average ordered moment of 3.06(9) μ_B per Fe atom on the Fe-dominated octahedral site, and no significant ordered moment on the second site. The magnetic Bragg scattering decreases to zero in the temperature interval $1.5 \leqslant T/K \leqslant 37(2)$. It is concluded that the partial cation ordering leads to the coexistence of a magnetically ordered spin system and a spin-glass system.

The magnetic susceptibility of many transition-metal oxides passes through a maximum value on cooling. This is often an indication that the compound has an antiferromagnetic low-temperature phase, but it is unwise to assume this on the basis of susceptibility data alone. It has become clear in recent years that, for a number of oxides, the spin system is static below the temperature of the susceptibility maximum but, in contrast to the situation in a true antiferromagnet, there is no long-range ordering of the atomic magnetic moments. The formation of this so-called spin-glass phase is most likely to occur when the compound contains more than one magnetic species[1] or when the particular combination of chemical composition and crystal structure leads to a degree of atomic disorder. Sr_2FeNbO_6,[2] in which paramagnetic Fe^{3+} and diamagnetic Nb^{5+} cations are distributed in a disordered manner over the six-coordinate sites of a pseudo-cubic perovskite structure, belongs to the latter category of compound. The concentration of magnetic cations (50%) on the sites of what is essentially a simple cubic cation sublattice is considerably greater than the percolation threshold (30.7%) for this non-frustrated system,[3] but susceptibility and hysteresis data suggest that Sr_2FeNbO_6 behaves as a spin glass below 32.5 K,[4] and there is no evidence of a transition to a phase showing long-range magnetic order. This behaviour is surprising in view of the fact that magnetically concentrated $LaFeO_3$ shows long-range order at temperatures as high as 750 K,[5] and theoretical models[6] predict a fall in T_N of only *ca.* 550 K when the Fe^{3+} concentration on the magnetic sublattice is reduced to 50%. Rodriguez *et al.*[4] explained this behaviour by postulating the existence of short-range structural ordering between Fe^{3+} and Nb^{5+}, but subsequent EXAFS and Mössbauer studies[7] failed to find any evidence for such an effect.

Following the work of Rodriguez *et al.*, we have reported behaviour similar to that of Sr_2FeNbO_6 in a wide range of mixed iron oxides with the general formula A_2FeMO_6 (A = Ca, Sr, Ba; M = Nb, Ta, Sb).[8,9] Of these compounds, Sr_2FeTaO_6 was studied in most detail. The X-ray diffraction pattern indicated that this compound is a cubic perovskite [a = 3.9664(9) Å] at room temperature with no (structural) ordering of the cations on the transition-metal sublattice.[9] On the basis of the non-Brillouin temperature dependence of the internal hyperfine field observed in the Mössbauer spectrum, and the observed magnetic hysteresis and thermal remanent magnetisation, we suggested that Sr_2FeTaO_6 is a spin glass below 23 K. In contrast, Sr_2FeSbO_6 crystallises in the monoclinic space group $P2_1/n$ and shows a partial ordering of the Fe^{3+} and Sb^{5+} cations over the six-coordinate sites.[8] The relatively low effective magnetic moment and the negative Weiss constant derived from magnetic susceptibility data ($\mu^{Fe} = 5.0\,\mu_B$, $\theta = -221$ K) suggested that strong, short-range, antiferromagnetic ordering is present in Sr_2FeSbO_6 in the temperature range $50 \leqslant T/K \leqslant 280$, although no difference between the field-cooled (FC) and zero-field-cooled (ZFC) magnetic susceptibility data was observed[8] in this temperature regime. However, such a difference was apparent below the susceptibility maximum at 36 K, suggesting that a spin-glass phase might exist at low temperatures, although the possibility of long-range magnetic order could not be ruled out. In order to establish unambiguously the nature of any long-range magnetic ordering in these two compounds, we have now collected neutron diffraction data on Sr_2FeMO_6 (M = Ta, Sb) over the temperature range $1.5 \leqslant T/K \leqslant 300$. The results of these experiments are described below.

Experimental

Polycrystalline samples (*ca.*10 g) of Sr_2FeMO_6 (M = Ta, Sb) were prepared as described previously.[8,9] Rietveld analyses[10] of X-ray powder diffraction patterns collected at room temperature in Bragg–Brentano geometry on a Siemens D5000 diffractometer (Cu-Kα_1 radiation, $5 \leqslant 2\theta/\text{degrees} \leqslant 120$, $\Delta 2\theta = 0.02^\circ$) established that the samples were monophasic. Constant-wavelength neutron powder diffraction data were collected using the instruments D1b and D2b at the ILL, Grenoble. The diffractometer D1b is equipped with a position-sensitive detector (PSD), having 400 detectors 0.2° apart in 2θ, making it possible to measure a low-resolution but complete diffraction pattern over the angular range $10 \leqslant 2\theta/\text{degrees} \leqslant 90$ without moving the detector. The instrument operates at a wavelength of 2.522 Å. During the course of our experiments on Sr_2FeSbO_6, a computer-controlled cryostat was used to ramp the sample temperature through the range $1.5 \leqslant T/K \leqslant 100$ at a constant rate of 9 K h^{-1}. The data were stored, and the

detectors reset to zero, every 15 min, giving a set of diffraction patterns with a temperature resolution of 2.25 K. The conventional diffractometer D2b operates at a neutron wavelength of 1.5938 Å (calibrated using X-ray data from our samples). During the course of each experiment (*ca.* 6 h), the bank of 64 detectors was used to collect data over the angular range $5 \leqslant 2\theta/\text{degrees} \leqslant 140$ with a 2θ stepsize of 0.05°. Data were collected on a weighed amount of sample contained in a cylindrical vanadium can (diameter = 10 mm) and mounted in a variable-temperature cryostat. All the neutron powder diffraction profiles collected in this program of experiments were analysed by the Rietveld profile analysis technique[10] using the GSAS suite of programs.[11] The data were not corrected for absorption. The following neutron scattering lengths were used: $b_{Sr} = 0.702$, $b_{Fe} = 0.954$, $b_{Ta} = 0.691$, $b_{Sb} = 0.564$ and $b_O = 0.5805 \times 10^{-14}$ m. The background was fitted using a shifted Chebyshev polynomial, and the shape of the Bragg peaks was described by a pseudo-Voigt function.

Results

Sr_2FeTaO_6

Inspection of a high-resolution neutron powder diffraction pattern collected from Sr_2FeTaO_6 at 280 K on D2b showed that, contrary to previous reports,[9] this compound is not a simple cubic perovskite at room temperature. The presence of additional Bragg peaks throughout the measured angular range suggested a larger unit cell, and the diffraction pattern was indexed in the orthorhombic space group *Pbnm* with unit-cell parameters $ca.\sqrt{2}\ a_p \times ca.\sqrt{2}\ a_p \times ca.2\ a_p$. This setting, often referred to as the $GdFeO_3$ structure type,[12] is consistent with our X-ray data in that it requires a disordered arrangement of Fe^{3+} and Ta^{5+} cations over a single crystallographic six-coordinate site. The refined values of the transformed unit-cell parameters confirmed that the magnitude of the orthorhombic strain was very small, and, because of this, there was a high correlation between certain structural parameters in our refinements. The agreement parameters resulting from the analysis of our neutron diffraction data [$R_{wp} = 9.07$; $R_p = 6.59$; $R_I = 5.55$; DW − d 0.179 (lower limit of 90% confidence level = 1.899[13]) $\chi_{rec}^2 = 11.66$] were all higher than might have been expected and the standard deviations on many of the atomic parameters were large. Furthermore, it was necessary to work with an overall temperature factor in order to stabilize the refinement, an unusual and undesirable occurrence in analysing neutron powder diffraction data collected at 280 K. An improved description of the crystal structure was achieved by performing a refinement using neutron and X-ray diffraction data simultaneously, thus making use of the complementarity of the two techniques. Thirty-nine variables were refined; seven atomic coordinates, four isotropic temperature factors, three lattice parameters and a set of profile parameters for each of the two data sets. The resulting atomic coordinates are listed in Table 1 and the most interesting bond lengths and bond angles are presented in Table 2. The values of the standard deviations on the coordinates are approximately half those obtained in the analysis based on the neutron data alone. The final agreement factors for the neutron profile used in the simultaneous refinement were $R_{wp} = 8.10$; $R_p = 5.91$; $R_I = 5.62$; DW − d 0.217; the value of χ_{red}^2 based on both data sets was 4.55.

A survey of Sr_2FeTaO_6 at 1.5 K on D1b suggested that there were no magnetic Bragg peaks in the low-angle region of the diffraction pattern, and this was confirmed by a high-resolution data set collected on D2b at 1.5 K. All the observed Bragg peaks could again be accounted for by an orthorhombic $GdFeO_3$ structure. The results of a profile analysis involving a total of 27 variables, including 11 atomic parameters, 5 background parameters and 4 peak-shape parameters are given in Table 3. Fig. 1 shows the final observed and calculated diffraction patterns. The resulting agreement parameters were as follows: $R_{wp} = 8.78$; $R_p = 6.59$; $R_I = 3.21$; DW − d 0.210 (lower limit of 90% confidence level = 1.901 [13]), $\chi_{red}^2 = 9.06$.

Sr_2FeSbO_6

The neutron powder diffraction profile of Sr_2FeSbO_6 collected on D2b at 290 K was consistent with the monoclinic space

Table 1 Structural parameters of Sr_2FeTaO_6 at 280 K (space group *Pbnm*)

atom	site	*x*	*y*	*z*	U_{iso}/Å^2
Sr	4c	0.0004(1)	0.0026(5)	1/4	0.0122(2)
Fe/Ta	4a	1/2	0	0	0.0048(2)
O(1)	8d	0.2530(9)	0.2522(9)	0.0168(3)	0.0109(3)
O(2)	4c	0.9569(3)	0.5160(3)	1/4	0.0079(5)

$a = 5.6204(3)$ Å; $b = 5.6161(3)$ Å; $c = 7.9266(3)$ Å; $V = 250.20(2)$ Å^3.

Table 3 Structural parameters of Sr_2FeTaO_6 at 1.5 K (space group *Pbnm*)

atom	site	*x*	*y*	*z*	U_{iso}/Å^2
Sr	4c	0.0008(9)	0.0097(8)	1/4	0.0067(3)
Fe/Ta	4a	1/2	0	0	0.0028(2)
O(1)	8d	0.2417(9)	0.244(1)	0.0201(3)	0.0077(4)
O(2)	4c	0.9526(6)	0.505(1)	1/4	0.0045(6)

$a = 5.6153(2)$ Å; $b = 5.6039(2)$ Å; $c = 7.9124(3)$ Å; $V = 248.98(2)$ Å^3.

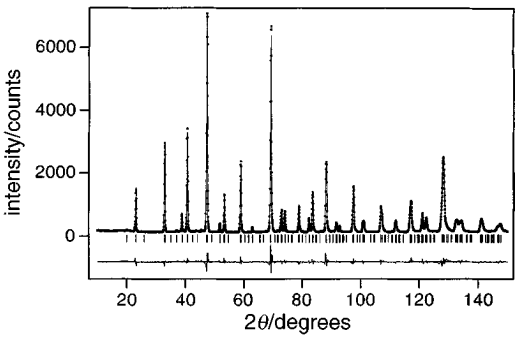

Fig. 1 Observed (dots), calculated (full line) and difference neutron powder diffraction patterns of Sr_2FeTaO_6 at 1.5 K (D2b data). Reflection positions are marked.

Table 2 Selected bond distances (Å) and angles (degrees) in Sr_2FeTaO_6 at 280 K

Sr−O(1)	2.705(5) (2×)	Sr−O(1)	2.881(5) (2×)
Sr−O(1)	2.720(5) (2×)	Sr−O(1)	2.924(5) (2×)
Sr−O(2)	2.571(6) (1×)	Sr−O(2)	2.744(6) (1×)
Sr−O(2)	2.894(6) (1×)	Sr−O(2)	3.051(6) (1×)
Fe/Ta−O(1)	1.988(5) (2×)	Fe/Ta−O(2)	1.9984(4) (2×)
Fe/Ta−O(1)	1.994(5) (2×)	shortest O−O	2.749(4)
O(1)−Fe/Ta−O(1)	90.30(1)	Fe/Ta−O(1)−Fe/Ta	172.26(13)
O(1)−Fe/Ta−O(2)	92.97(13)	Fe/Ta−O(2)−Fe/Ta	165.13(18)
O(1)−Fe/Ta−O(2)	90.77(13)		

group $P2_1/n$ which permits (partial) ordering of Fe^{3+} and Sb^{5+} over the octahedrally coordinated cation sites. During the course of the structure refinement, the $Fe^{3+}:Sb^{5+}$ distribution over these sites was refined within the constraints that the sites remained fully occupied and that the overall $Fe^{3+}:Sb^{5+}$ ratio remained at 1:1. The isotropic temperature factors of these two sites were constrained to be equal, as were those associated with the three crystallographically distinct oxygen atoms. This is another pseudo-symmetric structure, and we again chose to take advantage of the complementarity of neutron and X-ray diffraction by performing a simultaneous refinement of two data sets. In the last cycles of refinement, 48 variables (including 16 atomic parameters, 4 lattice parameters and 2 sets of profile parameters) were refined. The final agreement factors for the neutron data were as follows: $R_{wp}=5.28$; $R_p=4.10$; $R_I=6.27$; DW−d 0.587 (lower limit of 90% confidence level = 1.905[13]); the value of χ_{red}^2 based on both data sets was 1.56. The values of the refined parameters are given in Table 4, with the corresponding bond lengths and angles in Table 5. Despite the use of the simultaneous refinement technique, the pseudo-symmetry present in the structure resulted in relatively large standard deviations on the bond lengths. The observed and calculated neutron diffraction patterns are shown in Fig. 2. The diffraction data collected on the diffractometer D1b at 1.5 K contained additional Bragg reflections indicative of the presence of long-range, type I antiferromagnetic ordering (Fig. 3). A magnetic structure of this kind can be considered to consist of an antiferromagnetic stacking of ferromagnetic cation sheets along the z axis of the unit cell. In order to elucidate the details of the magnetic structure, we performed a Rietveld analysis using the free-ion form factor[14] of Fe^{3+} to describe the angular dependence of the magnetic scattering amplitude. There was no evidence of any major change in the crystal structure between 290 and 1.5 K, and, in view of the limited number of Bragg peaks in the D1b data set, the atomic parameters were held constant at the values determined at 290 K. Refinement of the appropriate profile parameters and the cation magnetic moment resulted in average values for the latter of 3.06(9) μ_B per Fe^{3+} on the B(1) site (79.5% Fe^{3+}) and 0.0(3) μ_B per Fe^{3+} on the B(2) site (20.5% Fe^{3+}). The ordered moment was constrained to lie along the x axis, but alignment along y is equally likely given the resolution of our data. The magnitudes of the magnetic moments are correlated with the chosen form factor, and may thus be in error by more than the statistical error quoted. Fig. 4 shows the final observed and calculated diffraction patterns at 1.5 K. The broad feature in the range $70 < 2\theta/\text{degrees} < 75$ which the model does not account for is

Table 4 Structural parameters of Sr_2FeSbO_6 at 290 K (space group $P2_1/n$)

atom	site	x	y	z	$U_{iso}/Å^2$
Sr	4e	−0.0007(8)	0.0019(8)	0.252(1)	0.0092(2)
B(1)	2d	1/2	0	0	0.0039(2)
B(2)	2c	0	1/2	0	0.0039(2)
O(1)	4e	0.249(2)	0.251(2)	0.019(4)	0.0096(2)
O(2)	4e	0.259(2)	0.254(2)	0.480(4)	0.0096(2)
O(3)	4e	0.9578(6)	0.515(1)	0.250(2)	0.0096(2)

Fractional occupancies on B(1): 0.795(6) Fe, 0.205(6) Sb; on B(2): 0.205(6) Fe, 0.795(6) Sb. $a=5.6132(5)$ Å; $b=5.5973(5)$ Å; $c=7.9036(7)$ Å; $\beta=90.01(1)$; $V=248.32(6)$ Å^3.

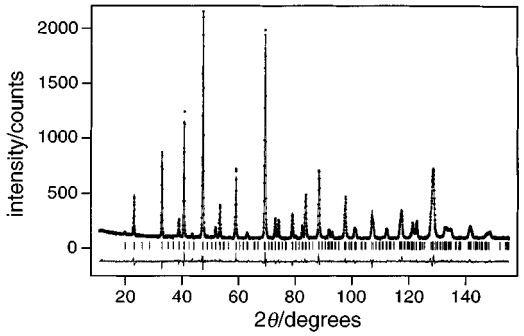

Fig. 2 Observed (dots), calculated (full line) and difference neutron powder diffraction patterns of Sr_2FeSbO_6 at 290 K (D2b data). Reflection positions are marked.

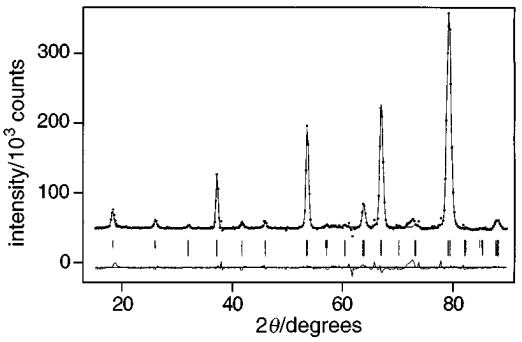

Fig. 4 Observed (dots), calculated (full line) and difference neutron powder diffraction patterns of Sr_2FeSbO_6 at 1.5 K (D1b data). Reflection positions are marked.

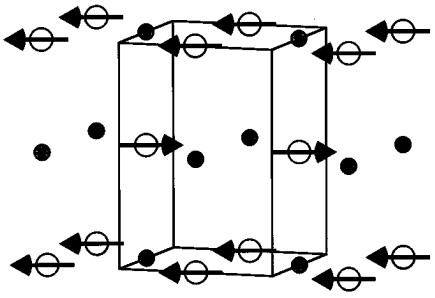

Fig. 3 The type I magnetic structure proposed for Sr_2FeSbO_6. Only the octahedrally coordinated cations are drawn: open circles B(1), shaded circles B(2).

Table 5 Selected bond distances (Å) and angles (degrees) of Sr_2FeSbO_6 at 290 K

Sr−O(1)	2.697(27)	Sr−O(2)	2.669(25)
Sr−O(1)	2.699(25)	Sr−O(2)	2.714(27)
Sr−O(1)	2.891(27)	Sr−O(2)	2.881(28)
Sr−O(1)	2.916(27)	Sr−O(2)	2.940(28)
Sr−O(3)	2.566(5)	Sr−O(3)	2.880(9)
Sr−O(3)	2.737(9)	Sr−O(3)	3.049(5)
B(1)−O(1)	1.995(10) (2×)	B(2)−O(1)	1.979(9) (2×)
B(1)−O(2)	2.006(9) (2×)	B(2)−O(2)	1.972(9) (2×)
B(1)−O(3)	1.994(14) (2×)	B(2)−O(3)	1.989(14) (2×)
B(1)−O(1)−B(2)	171(2)	B(1)−O(3)−B(2)	165.5(2)
B(1)−O(2)−B(2)	170(2)		

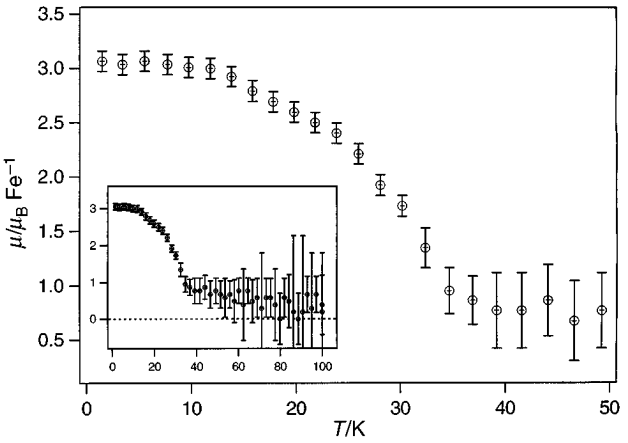

Fig. 5 Average magnetic moment of Fe^{3+} on the B(1) site in Sr_2FeSbO_6 as a function of the temperature

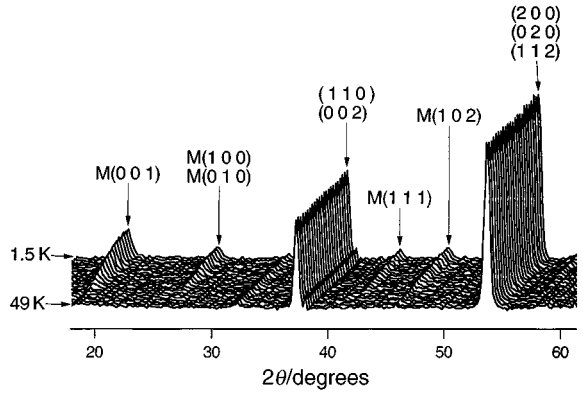

Fig. 6 Neutron diffraction patterns (D1b) of Sr_2FeSbO_6 as a function of temperature. Magnetic reflections are labelled 'M'.

thought to be instrumental in origin; it was present in all the profiles collected on D1b, but absent from the data collected on the same sample on D2b. Diffraction patterns collected during computer-controlled warming of the sample in the temperature range $1.5 \leqslant T/K \leqslant 100$ indicated that the magnetic structure remained type I until long-range magnetic order was lost altogether. These data were therefore analysed in a similar manner to that described above, although the ordered magnetic moment of the cations on the B(2) site was fixed at zero. In all cases the agreement factor R_{wp} fell to less than 4%. The temperature dependence of the resulting average moments on the B(1) site is plotted in Fig. 5. The value of the ordered moment decreases smoothly in the temperature range $1.5 \leqslant T/K \leqslant 37(2)$, above which it takes an approximately constant value which is within 3σ of zero. Visual inspection of the diffraction patterns presented in Fig. 6 suggests that the non-zero value refined at $T \geqslant 39$ K results from an attempt to fit background noise, thus defining the sensitivity limit of our measurements at *ca.* 1 μ_B.

Discussion

Neutron diffraction has shown that our previous description[9] of Sr_2FeTaO_6 as a simple cubic perovskite was wrong. The symmetry was previously overestimated because the deviation from high symmetry is caused almost entirely by a relatively small displacement of oxide ions from their ideal positions, and X-rays are therefore insensitive to the change. The revised crystal structure described above is common among perovskites, including those which contain more than one transition-metal species,[15] and the bond lengths in Table 2 are unexceptional. The disordered distribution of Fe and Ta atoms over one crystallographic site demonstrates that their cations do not differ sufficiently in size or charge for an ordered arrangement to be significantly more stable. The situation is different in Sr_2FeSbO_6, where ordering is present to a considerable extent, presumably because of the smaller size of Sb^{5+}. This reduction is apparent in the bond lengths listed in Table 5. The actual degree of ordering calculated in the simultaneous refinement of neutron and X-ray diffraction data [0.795(2)] is in excellent agreement with that deduced previously[8] from Mössbauer data [0.78(2)]. The ordering of the cations over the six-coordinate B sites, and the consequent displacements of the oxide ions, lowers the symmetry of the structure to monoclinic, but Sr_2FeSbO_6 can still be thought of as a pseudo-cubic perovskite.

We previously described Sr_2FeTaO_6 as a spin glass on the basis of susceptibility and Mössbauer data. The absence of magnetic Bragg peaks in the low-temperature neutron diffraction pattern proves that there is no long-range magnetic order in this compound below the susceptibility maximum at 23 K, despite the presence of a hyperfine field in the Mössbauer data. This confirms that the magnetic moments of the Fe^{3+} cations are disordered, despite being static (on the experimental timescale), and justifies the classification of this compound as a spin glass. The origin of this behaviour is still not clear. The transition-metal sublattice in the perovskite structure is not frustrated if only nearest-neighbour (NN) interactions are considered. One possibility is that frustration is introduced by competition between NN and next-nearest-neighbour (NNN) interactions. The latter will be weaker than the former, but they are more numerous (12:6). However, estimates of the ratio of the exchange constants, J_{NNN}/J_{NN}, in perovskite fluorides are only of the order 1/200,[16] and even allowing for the substantial increase in covalent overlap in a corresponding oxide, this argument is not entirely convincing. It is also possible that the answer lies in the presence of antiferromagnetic domains which are small when measured on the length-scale of a diffraction experiment. We are presently carrying out experiments and calculations to explore this possibility further.

The sensitivity of the magnetic properties to the degree of (chemical) cation ordering on the six-coordinate sites is demonstrated by the markedly different magnetic behaviour of Sr_2FeSbO_6. The susceptibility and Mössbauer data[8] enabled us to determine that magnetic frustration was present in this compound, but the presence of partial cation ordering led us to draw parallels with $SrLaNiSbO_6$,[17] and we suggested that a backbone of magnetically ordered spins might establish itself in Sr_2FeSbO_6, with clusters of frustrated spins, not connected to the backbone, also being present. The results of our neutron diffraction experiments support this explanation. The refined value of the average ordered magnetic moment per Fe^{3+} cation [3.06(9) μ_B] on the B(1) site is considerably lower than that observed in an ideal antiferromagnetic oxide of Fe^{3+} (*ca.* 4.4 μ_B[18]), even after allowance has been made for possible errors in the form factor, thus suggesting that only *ca.* 70% of the Fe^{3+} cations on these sites belong to the magnetic backbone. Alternatively, a higher percentage could be coupled, but with an imperfect alignment of the spin vectors. A third explanation is that the antiferromagnetic domain size is becoming small enough to reduce the observed moment. In the first two cases an unaligned spin component might contribute to the hysteresis observed in the magnetic susceptibility, while domain growth in a field would produce the same effect. The adoption of a type I magnetic structure implies that the most significant antiferromagnetic superexchange coupling takes place between cations separated by $\sqrt{2}a_0$; that is, between NNN transition-metal sites. The magnetic structure is thus consistent with the crystal structure in that $\sqrt{2}a_0$ is the distance between pairs of B(1) sites, which are both likely (63%) to be occupied by Fe; the B(1)—B(2) distance is shorter (a_0), but

the probability of adjacent B(1) and B(2) sites both being occupied by Fe is only 16%. In other words, each Fe^{3+} cation on a B(1) site is likely to be surrounded by (12×0.795) Fe^{3+} cations on NNN sites, but only (6×0.205) Fe^{3+} cations on NN sites. Our neutron diffraction results show that the concentration (20%) of Fe atoms present on the B(2) sites is too low for them to take part in any long-range magnetic ordering. However, the Mössbauer data do not show any evidence for a paramagnetic component at 4.2 K. It is not uncommon for frustrated spin systems to show spin freezing at low temperatures and the apparent lack of a finite moment on the B(2) site prompts us to assume that these atoms are indeed frustrated and contribute to the spin-glass component which the susceptibility data show to be present in the sample (a true antiferromagnet cannot show the observed divergence of the FC and ZFC susceptibilities). The temperature dependence of the magnetic Bragg scattering (Fig. 6) shows that the long-range magnetic ordering is lost at 37(2) K. Consideration of these data along with the magnetic susceptibility data[8] then shows that the glass-transition temperature and the Néel point are coincident, within experimental error.

The neutron diffraction experiments described above, considered in conjunction with Mössbauer and susceptibility data, have allowed us to build up a self-consistent description of the magnetic properties of Sr_2FeTaO_6 and Sr_2FeSbO_6. The former is a spin glass, with no long-range magnetic order present above 1.5 K, whereas an ordered backbone of spins and a spin-glass fraction coexist in the latter. In both cases there is evidence to suggest that the magnetic interactions between cations on NNN sites may be strong enough to influence the properties of the compound, an observation which urges caution in the use of models which rely on NN interactions to explain the properties of simple perovskite structures. However, we emphasise that the importance of NNN interactions is not proven in Sr_2FeTaO_6, and that alternative explanations, for example the presence of small antiferromagnetic domains, must be explored. We ascribe the variation in behaviour between Sr_2FeTaO_6 and Sr_2FeSbO_6 to the differing degrees of structural order on their transition-metal sublattices, an observation that demonstrates once again how structural chemistry can control solid-state physics.

We are grateful to J. P. Hodges, P. G. Radaelli and B. Ouladdiaf for experimental assistance, and to EPSRC for financial support.

References

1 S. H. Kim and P. D. Battle, *J. Solid State Chem.*, 1995, **114**, 174.
2 M. F. Kupriyanov and E. G. Fesenko, *Sov. Phys. Crystallogr.*, 1962, **6**, 639.
3 M. F. Sykes and J. W. Essam, *Phys. Rev. A*, 1964, **133**, 310.
4 R. Rodriguez, A. Fernandez, A. Isalgue, J. Rodriguez, A. Labarta, J. Tejada and X. Obradors, *J. Phys. C: Solid State Phys.*, 1985, **18**, L401.
5 W. C. Koehler and E. O. Wollan, *J. Phys. Chem. Solids*, 1957, **2**, 100.
6 D. J. Breed, K. Gilijamse, J. W. E. Sterkenburg and A. R. Miedema, *J. Appl. Phys.*, 1970, **41**, 1267.
7 T. C. Gibb, *J. Mater. Chem.*, 1993, **3**, 441.
8 P. D. Battle, T. C. Gibb, A. J. Herold and J. P. Hodges, *J. Mater. Chem.*, 1995, **5**, 75.
9 P. D. Battle, T. C. Gibb, A. J. Herod, S-H. Kim and P. H. Munns, *J. Mater. Chem.*, 1995, **5**, 865.
10 H. M. Rietveld, *J. Appl. Crystallogr.*, 1969, **2**, 65.
11 A. C. Larson and R. B. von Dreele, General Structure Analysis System (GSAS), Los Alamos National Laboratories, Report LAUR 86-748, 1990.
12 S. Geller, *J. Chem. Phys.*, 1956, **24**, 1236.
13 R. J. Hill and H. D. Flack, *J. Appl. Crystallogr.*, 1987, **20**, 356.
14 R. E. Watson and A. J. Freeman, *Acta Crystallogr.*, 1961, **14**, 27.
15 P. D. Battle and C. W. Jones, *Mater. Res. Bull.*, 1987, **22**, 1623.
16 L. J. D. Jongh and A. R. Miedema, *Adv. Phys.*, 1974, **23**, 1.
17 M. P. Attfield, P. D. Battle, S. K. Bollen, T. C. Gibb and R. J. Whitehead, *J. Solid State Chem.*, 1992, **100**, 37.
18 B. C. Tofield and B. E. F. Fender, *J. Phys. Chem. Solids*, 1970, **31**, 2741.

Paper 6/07083C; *Received* 17*th October*, 1996